

End-to-End Label Uncertainty Modeling in Speech Emotion Recognition using Bayesian Neural Networks and Label Distribution Learning

Navin Raj Prabhu, *Student Member, IEEE*, Nale Lehmann-Willenbrock, *Non-Member, IEEE*,
and Timo Gerkman, *Senior Member, IEEE*,

Abstract—To train machine learning algorithms to predict emotional expressions in terms of arousal and valence, annotated datasets are needed. However, as different people perceive others' emotional expressions differently, their annotations are per se subjective. For this, annotations are typically collected from multiple annotators and averaged to obtain ground-truth labels. However, when exclusively trained on this averaged ground-truth, the trained network is agnostic to the inherent subjectivity in emotional expressions. In this work, we therefore propose an end-to-end Bayesian neural network capable of being trained on a distribution of labels to also capture the subjectivity-based label uncertainty. Instead of a Gaussian, we model the label distribution using Student's t -distribution, which also accounts for the number of annotations. We derive the corresponding Kullback-Leibler divergence loss and use it to train an estimator for the distribution of labels, from which the mean and uncertainty can be inferred. We validate the proposed method using two in-the-wild datasets. We show that the proposed t -distribution based approach achieves state-of-the-art uncertainty modeling results in speech emotion recognition, and also consistent results in cross-corpora evaluations. Furthermore, analyses reveal that the advantage of a t -distribution over a Gaussian grows with increasing inter-annotator correlation and a decreasing number of annotators.

Index Terms—Emotional expressions, annotations, Bayesian neural networks, label distribution learning, end-to-end, speech emotion recognition, uncertainty, subjectivity, t -distributions, Kullback-Leibler divergence loss



1 INTRODUCTION

Emotions are typically studied as emotional expressions that others subjectively perceive and respond to [1], [2]. A common theoretical backdrop for analyzing emotions is the two-dimensional pleasure and arousal framework [3], which describes emotional expressions along two continuous, bipolar, and orthogonal dimensions: pleasure-displeasure (*valence*) and activation-deactivation (*arousal*). One way in which emotions become expressed in social interactions, and therefore accessible for social signal processing (SSP), concerns speech signals. Speech emotion recognition (SER) research spans roughly two decades [2], with ever improving state-of-the-art techniques. As a consequence, research on SER has shown increasing prominence in high-critical and socially relevant domains, such as health, security, and employee well-being [2], [4], [5].

In this work, we tackle the problem of recognising emotional expressions using speech signals, in terms of *time*- and *value*-continuous arousal and valence. A crucial challenge when studying emotional expressions is that their annotations in terms of arousal and valence are per se *subjective* because different people perceive others' emotional expressions differently [2], [5]. To address this, these annotations

are typically collected by multiple annotators and consensus on ground-truth is reached using techniques such as average scores [6], majority voting [6], or evaluator-weighted mean (EWE) [7]. These techniques in principle can lead to loss of valuable information on the inherent subjective nature of emotional expressions, and also tend to mask less prominent emotional traits [5]. In the context of *reliability* in real-world applications, it is required for SER systems to not only model ground-truth labels but also account for subjectivity [2], [8]. Moreover, by also capturing subjectivity, SER systems can be efficiently deployed in human-in-the-loop solutions, and aid in the development of algorithms for active learning, co-training, and curriculum learning [5].

We adopt an *end-to-end* framework for modeling time- and value-continuous emotional expressions. Common SER approaches rely on hand-crafted features to model emotion labels [9], [10]. Recently, end-to-end architectures have been shown to deliver state-of-the-art emotion predictions [11]–[13], by *learning* features rather than relying on hand-crafted features. For modeling *subjectivity* in emotions, it has been conjured that end-to-end learning also promotes learning subjectivity dependent representations [14].

Uncertainty in machine learning (ML) is studied under two categories. *Label uncertainty*, or aleatoric uncertainty, captures noise inherent in the data-samples, such as sensor noise or label noise [15], [16]. The label uncertainty *cannot* be reduced even if more data-samples are collected. Whereas, *model uncertainty*, or epistemic uncertainty, accounts for the uncertainty in model parameters, and the resulting uncertainty *can* be explained given enough data-samples [15]–[17]. Label uncertainty has been further categorized into

- Navin Raj Prabhu and Timo Gerkman are with the Signal Processing Lab, Universität Hamburg, Germany, 20146. E-mail: navin.raj.prabhu@uni-hamburg.de, timo.gerkman@uni-hamburg.de
- Nale Lehmann-Willenbrock is with the Department of Industrial and Organizational Psychology, Universität Hamburg, Germany, 20146. E-mail: nale.lehmann-willenbrock@uni-hamburg.de

This work was supported by the Landesforschungsförderung Hamburg (LFF-FV79), as part of the research unit "Mechanisms of Change in Dynamic Social Interactions".

homoscedastic uncertainty, which remains constant across data-samples, and *heteroscedastic* uncertainty, whose uncertainty depends on the respective data-sample. This work specifically aims to model the heteroscedastic label uncertainty, henceforth simply mentioned as *label uncertainty*, that corresponds to the *inherent subjectivity in emotion annotations*.

We propose to use *Bayes by Backpropagation* (BBB), a Bayesian neural network (BNN) technique, for capturing label uncertainty. In ML, stochastic and probabilistic models have mainly been used for uncertainty modeling, through ensemble learning [18], encoder-decoder architectures [19], neural processes [20], [21], and BNNs [22]–[24]. Of which, the Bayesian frameworks show improved performance over non-Bayesian baselines [15], [25], making BNNs such as Monte-Carlo dropout [22] and BBB [23] promising candidates for label uncertainty in SER. BBB uses *simple gradient updates* to optimize weight distributions for *stochastic outputs*, thereby are capable of being trained on a distribution of annotations and suitable for end-to-end architectures.

With BBB capable of being trained on a distribution of annotations, we capture label uncertainty using the *label distribution learning* (LDL) technique [25], by leveraging Kullback-Leibler (KL) divergence-based loss functions. Subjective annotations of emotion create a label distribution to represent the subjectivity in emotions [5]. For simplicity, histograms [5], and Gaussians [26] have been the choices of distributional families. However, Gaussians and histograms with *limited observations* are not well justified [27]–[29], as the central limit theorem (CLT) which primarily backs them does not hold with insufficient numbers of samples [30]. Publicly available SER datasets commonly comprise of only three to six annotations [31]–[35], and well agree that gaining more annotations is expensive and resource inefficient [5], [36]. To tackle this, in this work, we model emotion annotation distributions as a Student’s *t*-distribution, or simply *t*-distribution, that also accounts for the number of annotations available while modeling [27].

In this paper, we present a BBB-based end-to-end architecture that uses LDL to model emotion annotations as a *t*-distribution. To this end, we derive a KL divergence loss for label uncertainty that quantifies distribution similarity between stochastic emotion predictions, modeled as a Gaussian distribution, and *ground-truth emotion annotations*, modeled as a *t*-distribution. Subsequently, we present analyses to reveal the benefits of using *t*-distribution over a Gaussian. We validate the proposed model in two in-the-wild datasets, AVEC’16 [37] and MSP-Conversation [31]. We show that the proposed model can aptly capture label uncertainty with state-of-the-art results in both the datasets, along with a robust loss curve. To emphasize the benefits of the *t*-distribution, we present experiments studying the impact of the number of emotion annotations available. Finally, we perform an ablation study to understand specific benefits of the respective modules in the architecture.

This work is based on two prior conference contributions [38], [39], which to the best of our knowledge are the first in the literature to use BBB and LDL in SER. These works were also the first to tackle the problem of limited emotion annotations from an ML perspective. While in [38], [39] we only validated the method in one dataset, and with limited experiments, in this extension, we additionally validate the

method in a larger and more complex dataset, the MSP-Conversation [31], along with cross-corpora evaluations. This extension is also the first in literature to present SER results in this novel dataset [31]. Existing analyses and experiments from [38], [39] were also extended to MSP-Conversation. Moreover, we performed additional experiments that include an experiment to understand the impact of the number of annotations available, and an ablation study. Code for the proposed model and loss function is available online ¹.

2 BACKGROUND AND RELATED WORK

2.1 Ground-truth labels

To handle subjectivity in emotional expressions, annotations $\{y_1, y_2, \dots, y_a\}$ for emotions are collected from several *a* annotators [33], [35]. The *ground-truth label* is then obtained as the mean m across all annotations from *a* annotators [40],

$$m = \frac{1}{a} \sum_{i=1}^a y_i. \quad (1)$$

Alternatively, the EWE, which weights annotations with inter-annotator correlations, has been proposed as the *gold-standard* \tilde{m} [7]. Both m and \tilde{m} based approximation of ground-truth leads to loss of information on subjectivity [5].

Traditional SER approaches, given a raw audio sequence of T frames $\mathcal{X} = [x_1, x_2, \dots, x_T]$, aim to estimate either the m_t or \tilde{m}_t for each time frame $t \in [1, T]$, referred to as \hat{m}_t . The concordance correlation coefficient (CCC) has been widely used as a loss function for this task [2]. For Pearson correlation r , the CCC between m and \hat{m} , for T frames is:

$$\mathcal{L}_{\text{CCC}}(m) = \frac{2r\sigma_m\sigma_{\hat{m}}}{\sigma_m^2 + \sigma_{\hat{m}}^2 + (\mu_m - \mu_{\hat{m}})^2}, \quad (2)$$

where $\mu_m = \frac{1}{T} \sum_{t=1}^T m_t$, $\sigma_m^2 = \frac{1}{T} \sum_{t=1}^T (m_t - \mu_m)^2$, and $\mu_{\hat{m}}$, $\sigma_{\hat{m}}^2$ are obtained similarly for \hat{m} .

2.2 Label uncertainty in SER

Alternative to exclusively modeling m_t or \tilde{m}_t , previous research has attempted to model ground truth that also explains inter-annotator disagreement, for example by means of soft labels [5] and entropy of disagreement [41]. Sridhar et al. [5] proposed an auto-encoder technique to jointly model soft- and hard-labels of emotion annotations, and subsequently estimate label uncertainty as the entropy on soft-labels. Fayek et al. [42] and Tarantino et al. [43] proposed to learn soft labels instead of m_t with improved performance. Steidl et al. [41] quantified label uncertainty using the entropy measure, and trained a model to minimize the difference in entropy between model outputs and annotator disagreement.

Label uncertainty has also been approached as a prediction task by estimating the moments of a distribution [9], [44]. Han et al. [9], [44] used a multi-task learning (MTL) framework to model the unbiased standard deviation s of *a* annotators as an auxiliary task,

1. <https://github.com/sp-uhh/label-uncertainty-ser>

$$s = \sqrt{\frac{1}{a-1} \sum_{i=1}^a (y_i - m)^2}. \quad (3)$$

Similarly, Dang et al. [45] directly capture the temporal dependencies in the annotation signals, by using multirate Gaussian mixture regression and Kalman filters. Sridhar et al. [10] introduced a Monte-Carlo (MC) dropout model to obtain uncertainty estimates from the distribution of stochastic outputs. However, the model is not explicitly trained on any label uncertainty estimate and hence can only capture the model uncertainty. A similar MC dropout was used by Rizos et al., [46] who propose a meta-learning framework that uses uncertainty estimates to potentially detect highly-uncertain samples and perform soft data selection for the training process.

Research efforts have also made to estimate emotion annotations as a distribution, using LDL [26], [38], [39], [47]. Foteinopoulou et al. [26] trained a MTL network using a KL divergence loss that models emotion annotations as a *uni-variate Gaussian* with mean m and unknown variance. Chou et al., [47] used LDL to convert perceptual evaluations into *histogram*-based distributional labels for training. In our preliminary work [38], we modeled emotion annotations as a *Gaussian* using BBB-based uncertainty modeling. Notwithstanding their improved performances, in [26], [38], [47], a *histogram* or a *Gaussian* assumption was made on emotion annotations, despite only having limited annotations. Apart from the apparent mathematical incorrectness of these assumptions for limited annotations, these approaches are susceptible to unreliable m and s for lower values of a and sparsely distributed annotations. In our subsequent work [39] and in this extension, we tackle this problem by modeling emotion annotation distribution as a *t-distribution* and show advantages over a Gaussian assumption.

2.3 On distributional assumptions

A Gaussian distribution $\mathcal{Y} \sim \mathcal{N}(\mu, \sigma^2)$ is a continuous probability distribution for a real-valued random variable y , with general form of its probability density function [28]

$$p(y | \mu, \sigma) = \frac{1}{\sigma\sqrt{2\pi}} e^{-\frac{1}{2}\left(\frac{y-\mu}{\sigma}\right)^2}. \quad (4)$$

The parameters μ and σ are the mean and standard deviation of the distribution, respectively. Due to its simplicity, Gaussians are often used to model random variables whose distributional family are unknown [23], [38]. Their importance is however backed by the CLT which only holds *with sufficient observations of the random variable* [30]. Due to resource constraints in collecting annotations, in most human-behaviour research [36] and in SER [31]–[34], we do not have sufficient annotations to assume a Gaussian on them. As this is a common challenge for label uncertainty, it is important for SER algorithms to account for *limited* annotations and model annotation distributions accordingly. Kotz and Nadarajah [27], and, Bishop and Nasrabadi [28], note that in scenarios of limited observations the *t-distribution* becomes more robust and realistic over a Gaussian.

Student's *t-distribution*, $\mathcal{Y}_t \sim \mathcal{N}(\nu, \mu, \sigma)$, arises when estimating the moments of a normally distributed population

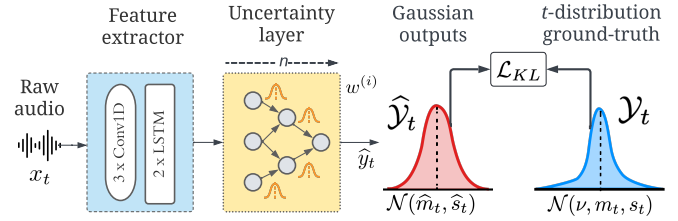


Fig. 1: Overview of proposed architecture and loss \mathcal{L}_{KL} . n : number of forward passes. $w^{(i)}$ and \hat{y}_t : stochastically sampled weight and realization of $\hat{\mathcal{Y}}_t$, at i^{th} forward pass.

in situations where the sample size is small [27], [48], with the probability density function given by [29], [49],

$$p(y | \nu, \mu, \sigma) = \frac{1}{B(\frac{1}{2}, \frac{\nu}{2})} \frac{1}{\sqrt{\nu\sigma^2}} \left(1 + \frac{(y - \mu)^2}{\nu\sigma^2}\right)^{-\frac{\nu+1}{2}}, \quad (5)$$

where ν denotes the degrees of freedom and $B(\cdot, \cdot)$ is the Beta function, for Gamma function Γ , formulated as,

$$B(i, j) = \frac{\Gamma(i)\Gamma(j)}{\Gamma(i+j)}. \quad (6)$$

The density function (5) is symmetric, and its overall shape resembles the bell shape of a normally distributed variable, except that it has heavier tails, meaning that it better captures values that fall far from its mean [27], [28]. The degree of freedom ν , also known as the normality parameter, controls the normality of the distribution, and is correlated with the σ parameter [27], [28]. The standard deviation σ in (5) is scaled by ν and is formulated as

$$\sigma = \sigma \sqrt{\frac{\nu}{\nu-2}} \text{ for } \nu > 2. \quad (7)$$

As ν increases, the *t-distribution* approaches the normal distribution [29].

3 PROPOSED LABEL UNCERTAINTY MODEL

In order to better represent subjectivity in emotional expressions, we propose to estimate the *emotion annotation distribution* \mathcal{Y}_t for each time-frame t , given raw audio x_t . While the true distributional family of subjectively perceived emotions \mathcal{Y}_t is unknown, for simplicity, we can assume that it follows a Gaussian distribution:

$$\mathcal{Y}_t \sim \mathcal{N}(m_t, s_t). \quad (8)$$

However, with only a limited number of samples, i.e. annotations, we argue that a Gaussian assumption is rather crude [27], [28]. Instead, we propose to model the emotion annotations as a *t-distribution*, with degrees of freedom ν :

$$\mathcal{Y}_t \sim \mathcal{N}(\nu, m_t, s_t). \quad (9)$$

Thus, the goal is to obtain an estimate $\hat{\mathcal{Y}}_t$ of \mathcal{Y}_t and infer both \hat{m}_t and \hat{s}_t from realizations of $\hat{\mathcal{Y}}_t$.

3.1 End-to-end DNN architecture

We propose an end-to-end architecture which uses a feature extractor to learn temporal-paralinguistic features from x_t , and an uncertainty layer to estimate \mathcal{Y}_t (see Fig. 1). The feature extractor, inspired from [11], consists of three Conv1D layers followed by two stacked long-short term memory (LSTM) layers. The uncertainty layer is devised using the BBB technique [23], comprising three BBB-based MLP.

3.2 Model uncertainty loss

Unlike a standard neuron which optimizes a deterministic weight w , the BBB-based neuron learns a probability distribution on the weight w by calculating the variational posterior $P(w|\mathcal{D})$ given the training data \mathcal{D} [23]. Intuitively, this regularizes w to also capture the inherent uncertainty in \mathcal{D} . Following [23], we parametrize $P(w|\mathcal{D})$ using a Gaussian $\mathcal{N}(\mu_w, \sigma_w)$. For non-negative σ_w , we re-parametrize the standard deviation $\sigma_w = \log(1 + \exp(\rho_w))$. Then, $\theta = (\mu_w, \rho_w)$ can be optimized using simple backpropagation.

For an optimized θ , the predictive distribution $\hat{\mathcal{Y}}_t$ for x_t , is given by $P(\hat{y}_t|x_t) = \mathbb{E}_{P(w|\mathcal{D})}[P(\hat{y}_t|x_t, w)]$, where \hat{y}_t are realizations of $\hat{\mathcal{Y}}_t$. Unfortunately, the expectation under the posterior of weights is intractable. To tackle this, [23] proposed to learn θ of a weight distribution $q(w|\theta)$, the variational posterior, that minimizes the Kullback-Leibler (KL) divergence with the true Bayesian posterior, resulting in the negative evidence lower bound (ELBO),

$$f(w, \theta)_{\text{BBB}} = \text{KL}[q(w|\theta)||P(w)] - \mathbb{E}_{q(w|\theta)}[\log P(D|w)]. \quad (10)$$

Stochastic outputs in BBB are achieved using multiple forward passes n with stochastically sampled weights w , thereby modeling $\hat{\mathcal{Y}}_t$ using the n stochastic estimates. To account for the stochastic outputs, (10) is approximated as,

$$\mathcal{L}_{\text{BBB}} \approx \sum_{i=1}^n \log q(w^{(i)}|\theta) - \log P(w^{(i)}) - \log P(D|w^{(i)}). \quad (11)$$

where $w^{(i)}$ denotes the i^{th} weight drawn from $q(w|\theta)$. The BBB window-size b controls how often new weights are sampled for time-continuous SER. The degree of uncertainty is assumed to be constant within this time period. During testing, the uncertainty estimate $\hat{\sigma}_t$ is the standard deviation of $\hat{\mathcal{Y}}_t$, and, \hat{m}_t is the realization \hat{y}_t obtained using the mean of the optimized weights μ_w . Obtaining \hat{m}_t using μ_w helps overcome the randomization effect of sampling from $q(w|\theta)$, which showed better performances in our case.

3.3 Label uncertainty loss

While (11) exclusively captures *model uncertainty*, the aim of this work is to also capture *label uncertainty*. For this, using LDL, inspired by [16], we introduce a *KL divergence-based loss* to fit our model to the annotation distribution \mathcal{Y}_t , both for a Gaussian (8), and a t -distribution (9).

3.3.1 Gaussian \mathcal{Y}_t KL divergence

For a Gaussian assumption on \mathcal{Y}_t (8), the label uncertainty loss, the KL divergence between two Gaussians $\mathcal{Y}_t \sim \mathcal{N}(\mu, \sigma^2)$ and $\hat{\mathcal{Y}}_t \sim \mathcal{N}(\hat{\mu}, \hat{\sigma}^2)$, is formulated as [28],

$$\mathcal{L}_{KL} = f(\mathcal{Y}_t||\hat{\mathcal{Y}}_t) = \log\left(\frac{\hat{\sigma}}{\sigma}\right) + \frac{\sigma^2 + (\mu - \hat{\mu})^2}{2\hat{\sigma}^2} - \frac{1}{2}. \quad (12)$$

The KL divergence is asymmetric, making the order of distributions crucial. In (12), we choose $\hat{\mathcal{Y}}_t$ to follow $\hat{\mathcal{Y}}_t$, for mean-seeking approximation rather than a mode-seeking one to capture the full distribution [50].

3.3.2 t -distribution \mathcal{Y}_t KL divergence

For \mathcal{Y}_t as a t -distribution (9), we derive the KL divergence between $\mathcal{Y}_t \sim \mathcal{N}(\nu, \mu, \sigma^2)$ and the Gaussian outputs $\hat{\mathcal{Y}}_t \sim \mathcal{N}(\hat{\mu}, \hat{\sigma}^2)$. Assuming a Gaussian on $\hat{\mathcal{Y}}$ is fair, as the number of stochastic outputs to model $\hat{\mathcal{Y}}$ can be controlled using n in (11). In this work, we intend to fix $n \geq 30$, as a t -distribution converges to a stable Gaussian with 30 samples [29], [49]. As a positive side effect, we result in deriving the KL divergence between a Gaussian and a t -distribution, in contrast to between two t -distributions, with the later involving mathematical complexities in calculating intractable expectations for a loss function.

For a Gaussian $\hat{\mathcal{Y}}$ (see (4)), and a t -distributed \mathcal{Y} (see (5)), the \mathcal{L}_{KL} is formulated as [51], [52],

$$\mathcal{L}_{KL} = f(\mathcal{Y}_t||\hat{\mathcal{Y}}_t) = H(\mathcal{Y}_t, \hat{\mathcal{Y}}_t) - H(\mathcal{Y}_t), \quad (13)$$

where $H(\cdot, \cdot)$ is the cross-entropy between two distributions, and $H(\cdot)$ is the entropy of a distribution. The cross-entropy term $H(\cdot, \cdot)$ in (13), using (4), can be further formulated as,

$$\begin{aligned} H(\mathcal{Y}_t, \hat{\mathcal{Y}}_t) &= - \int \mathcal{Y}_t(y) \log \hat{\mathcal{Y}}_t(y) dy \\ &= \frac{1}{2} \log(2\pi\hat{\sigma}^2) + \int \mathcal{Y}_t(y) \left(\frac{(y - \hat{\mu})^2}{2\hat{\sigma}^2} \right) dy \\ &= \frac{1}{2} \log(2\pi\hat{\sigma}^2) + \frac{1}{2\hat{\sigma}^2} \left[\int \mathcal{Y}_t(y) y^2 dy - 2\hat{\mu} \int \mathcal{Y}_t(y) y dy \right. \\ &\quad \left. + \hat{\mu}^2 \int \mathcal{Y}_t(y) dy \right]. \quad (14) \end{aligned}$$

Noting that $\int \mathcal{Y}_t(y) y^2 dy = \mu^2 + \sigma^2$, $\int \mathcal{Y}_t(y) y dy = \mu$, and $\int \mathcal{Y}_t(y) dy = 1$, where μ and σ are parameters of the t -distribution $\mathcal{Y}_t, p(y | \nu, \mu, \sigma)$, the equation (14) becomes,

$$\begin{aligned} &= \frac{1}{2} \log(2\pi\hat{\sigma}^2) + \frac{1}{2\hat{\sigma}^2} \left[\sigma^2 + \mu^2 - 2\hat{\mu}\mu + \hat{\mu}^2 \right] \\ &= \frac{1}{2} \log(2\pi\hat{\sigma}^2) + \frac{\sigma^2 + (\mu - \hat{\mu})^2}{2\hat{\sigma}^2} \quad (15) \end{aligned}$$

Finally, using (15) in (13), our proposed KL divergence is

$$\mathcal{L}_{KL} = \frac{1}{2} \log(2\pi\hat{\sigma}^2) + \frac{\sigma^2 + (\mu - \hat{\mu})^2}{2\hat{\sigma}^2} - H(\mathcal{Y}_t). \quad (16)$$

We implement (16) as a custom loss function by extending the `studentT` pytorch sub-package [53].

3.3.3 Comparing Gaussian and t -distribution loss

While the two loss-functions (12) and (16) have their second term in common, two differences can be noted. Firstly, as (12) calculates the divergence between two similar distributions, \mathcal{Y}_t and $\hat{\mathcal{Y}}_t$, (12) includes the logarithm of the ratio between the two Gaussian's standard deviation in its formulation. However, in (16), the deviations of \mathcal{Y}_t and $\hat{\mathcal{Y}}_t$ are separately quantified using terms $\frac{1}{2} \log(2\pi\sigma^2)$ and $H(\mathcal{Y}_t)$, respectively. Secondly, (16) is dependent on the number of annotators through scaling $\hat{\sigma}_t$ with normality factor ν (7).

To further understand the advantages of the t -distribution \mathcal{L}_{KL} (16) over the Gaussian \mathcal{L}_{KL} (12), we plot

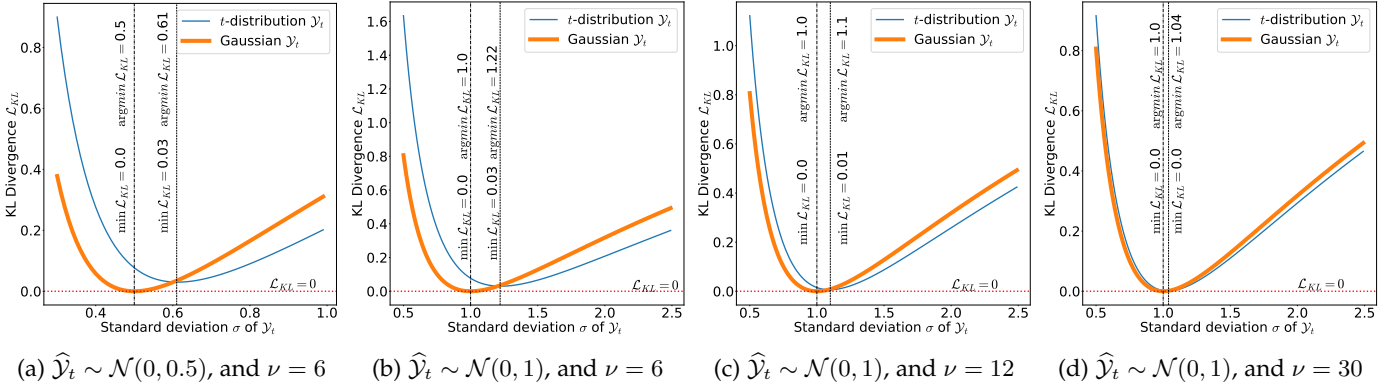


Fig. 2: Analysis of the t -distribution based KL divergence \mathcal{L}_{KL} (16), in comparison with Gaussian \mathcal{L}_{KL} (12).

the \mathcal{L}_{KL} values as a function of varying σ of \mathcal{Y}_t , for (16) and (12). We perform this analysis under four different scenarios, by varying parameters $\hat{\sigma}$ and ν , i) Figure 2a for scenario $\hat{\sigma} = 0.5$ and $\nu = 6$, ii) Figure 2b for scenario $\hat{\sigma} = 1.0$ and $\nu = 6$, iii) Figure 2c for scenario $\hat{\sigma} = 1.0$ and $\nu = 12$, and, iv) Figure 2d for scenario $\hat{\sigma} = 1.0$ and $\nu = 30$.

From Figure 2, firstly, we see that \mathcal{L}_{KL} behaves differently when the ground-truth \mathcal{Y}_t is modeled as a t -distribution (16), in comparison to the Gaussian assumption (12). Specifically, from Figure 2a, for $\hat{\sigma} = 0.5$ and $\nu = 6$, we see that the minimum \mathcal{L}_{KL} (16) is achieved only at $\sigma = 0.61$, in contrast to the Gaussian (12) $\hat{\sigma} = \sigma = 0.5$. While the Gaussian attempts exactly fitting the model to the ground-truth $\sigma = 0.5$, the t -distribution tries to fit on a more relaxed $\sigma = 0.61$ by also considering the reduced degree of freedom $\nu = 6$. This behaviour is similar to the confidence intervals calculation using a t -distribution [54, Section 9.5], where relaxation on σ is noted with respect to ν . Moreover, [28] associate this relaxed σ towards the increased robustness of the t -distribution to outliers and sparse distributions.

Secondly, we note that the observed relaxation on σ is dependent on two factors, 1) the standard-deviation of the stochastic outputs $\hat{\sigma}$, and 2) the degree of freedom of the ground-truth ν . From figures 2a and 2b, we see that, while ν is constant, the relaxation on σ increases along with an increase in $\hat{\sigma}$. At $\hat{\sigma} = 0.5$ a relaxation of 0.11 is made by t -distribution (16) from 0.5 to 0.61, while a larger relaxation of 0.22 is made for $\hat{\sigma} = 1.0$. Similarly, from figures 2c and 2d, we see that, while $\hat{\sigma}$ is constant, as ν increases the relaxation on σ decreases. That is, the t -distribution (16) starts behaving similar to a Gaussian, inline with literature that states that as the degree of freedom ν of t -distribution increases, the distribution converges into a Gaussian [27], [29], [49]. This is also inline with our initial motivation behind using the t -distribution, which we expected to account for the number of annotators ν while fitting on annotation distribution \mathcal{Y} .

From an ML and SER perspective, from Figure 2, we note several benefits of t -distribution based loss term towards label uncertainty modeling. Firstly, training on a t -distribution \mathcal{L}_{KL} (16) leads to training on a relaxed s_t , and thereby can lead to better capturing of the whole ground-truth label distribution. Moreover, the resulting loss function is mathematically more solid than a Gaussian assumption, when less than *thirty* annotations are available, which holds for all current SER databases we are aware of. Secondly,

we note that the t -distribution \mathcal{L}_{KL} (16) values are always higher for lower values of σ and $\hat{\sigma}$, in all cases. This, in comparison to the Gaussian \mathcal{L}_{KL} (12), might lead to larger penalization of the model through the \mathcal{L}_{KL} loss, and may thereby promote better and quicker convergence during training. Finally, the t -distribution \mathcal{L}_{KL} (16) can also adapt to different datasets by also accounting for the number of annotations available during training.

3.4 Training loss

The proposed end-to-end uncertainty loss is formulated as,

$$\mathcal{L} = (1 - \mathcal{L}_{CCC}(m)) + \mathcal{L}_{BBB} + \alpha \mathcal{L}_{KL}. \quad (17)$$

Intuitively, $\mathcal{L}_{CCC}(m)$ optimizes for mean predictions m , \mathcal{L}_{BBB} optimizes for BBB weight distributions, and \mathcal{L}_{KL} optimizes for the label distribution \mathcal{Y}_t . For $\alpha = 0$, the model only captures model uncertainty (MU). For $\alpha = 1$, the model also captures *label uncertainty (+LU)*. $\mathcal{L}_{CCC}(m)$ is used as part of \mathcal{L} to achieve faster convergence and jointly optimize for mean predictions. Including $\mathcal{L}_{CCC}(m)$ might lead to better optimization of the feature extractor [11], [55].

4 EXPERIMENTAL SETUP

4.1 Dataset

To validate our proposed methodology, we use two publicly available in-the-wild datasets, with time- and value-continuous annotations for arousal and valence. Firstly, the AVEC'16 [37] version of the RECOLA dataset [33], which has 2.15hrs of annotated dyadic interactions. Secondly, the MSP-Conversation dataset, which has 15.15hrs of annotated interactions with groups of 2-7 interlocutors.

4.1.1 AVEC'16 dataset

The dataset consists of arousal and valence annotations by $a = 6$ annotators at 40 ms frame-rate, or 25 frames per second (fps). As illustrated in Figure 3, in the AVEC'16 dataset [37], arousal and valence annotations are distributed on average with $\mu_m = 0.01$ and $\mu_m = 0.11$, and $\mu_s = 0.23$ and $\mu_s = 0.14$, respectively, where $\mu_s = \frac{1}{T} \sum_{t=1}^T s_t$. This reveals the significant level of subjectivity present in the dataset, where s_t distributions are heavy-tailed with usually high s_t and μ_s . The dataset is divided into speaker disjoint

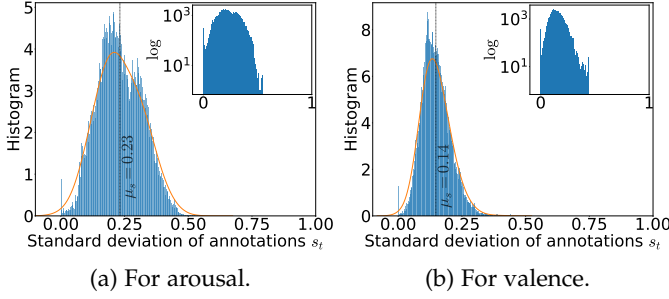


Fig. 3: Histogram of standard deviations s_t in AVEC'16.

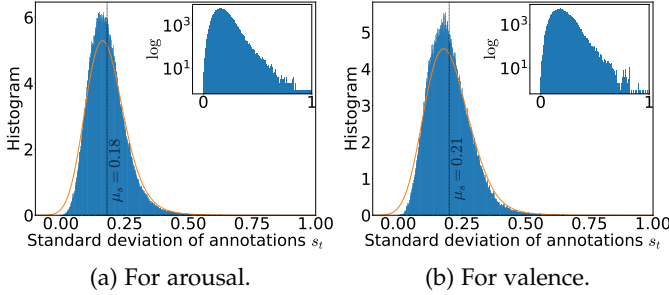


Fig. 4: Histogram of standard deviations s_t in MSPConv.

partitions for training, development and testing, with nine 300 s recordings each. As the annotations for the test partition are not publicly available, all results are computed on the development partition.

4.1.2 MSP-Conversation dataset

The MSP-Conversation, or simply *MSPConv*, is approximately 7 times larger than AVEC'16, comprising of in-the-wild podcasts. The wide range of podcast recordings leads to high variability in-terms of population size, group size, and more importantly its emotional content [31], [32], making the MSPConv a more complex dataset to model.

The dataset consists of time- and value-continuous annotations for arousal and valence, performed by at least $a = 6$ annotators at ≈ 16 ms frame-rate, or 60 fps, however not uniform in all cases [31]. For uniform sampling rate, we perform median filtering with a window-size of 500ms, as suggested in [31]. To keep the sampling rate consistent between the two datasets, for cross-corpora evaluations, we use a step-size of $1/25$ s in median filtering. A local normalization, i.e., for each annotated sequence and for each annotator, was performed using zero-mean unit-deviation normalization [33], similar to AVEC'16. As illustrated in Figure 4, in the MSPConv dataset [31], arousal and valence annotations are distributed on average with $\mu_m = -0.01$ and $\mu_m = 0.00$, and $\mu_s = 0.18$ and $\mu_s = 0.21$, respectively. Further revealing the complexity of MSPConv, when comparing figures 3 and 4, we see that the level of subjectivity in MSPConv is higher than the AVEC'16 dataset, where the distribution tail is more heavy in MSPConv. The heavy tails are more clear in the log-histogram plotted along in Fig. 4.

From preliminary experiments, it was noted that the arousal and valence annotations, specially from particular annotators—001, 007, and 009, were prone to periodic distortion noises. This could have originated due to any techni-

cal error or a human-error by the annotator. Directly training on these noisy annotations degraded the performance of all the models in comparison. Ignoring them might lead to loss of information, and also result in reduced number of available annotations to derive ground-truth. To reduce this periodic distortions and still retain the inherent annotation information, we use a low-pass filter [56] with a cut-off frequency of 0.25Hz. The cut-off frequency was tuned using a Fourier analysis [57] followed by a qualitative analysis on the filtered annotations. Filtering was performed only on annotations *with periodic distortions*, i.e., from the three annotators—001, 007, and 009.

4.2 Baselines and Proposed model versions

E2E Baseline: The *E2E Baseline* uses the same end-to-end framework as our proposed model, but with a simple multi-layer perceptron layer instead of the uncertainty layer (see Fig. 1). The model does not capture any form of uncertainty, and is exclusively trained on the $\mathcal{L}_{CCC}(m)$ loss (2).

MTL Baselines: From [9], [44], as the baselines, we use the perception uncertainty (*MTL PU*) and single-task models (*STL*). The MTL PU is a label uncertainty model that also models s_t as an auxiliary task. The STL does not capture uncertainty and is exclusively trained on $\mathcal{L}_{CCC}(m)$ (2). For a fair comparison, we reimplemented these baselines and tested them in our test bed. Crucially, the reimplementation also enables us to compare the models in-terms of their s estimates, which were not presented in Han et al.'s work [9]. The only difference between Han et al.'s test bed [9] and ours is the post-processing pipeline, where [9] used the AVEC'16 post-processing pipeline while we use the median filtering [11] as the sole post-processing technique.

Proposed BBB-LDL versions: We use three versions of the proposed label uncertainty model. Firstly, the *Model Uncertainty (MU)* version, which share the same DNN architecture as the other BBB version but trained on (17) with $\alpha = 0$. Secondly, the *Label Uncertainty (MU+LU)* version with also captures the label uncertainty and trained on (17) with $\alpha = 1$. The MU+LU version however makes a Gaussian assumption on \mathcal{Y}_t , thereby \mathcal{L}_{KL} follows (12). Finally, the *t-distribution Label Uncertainty (t-LU)* version, which is trained on the same loss function (17) but models \mathcal{Y}_t as a *t*-distribution, and \mathcal{L}_{KL} follows (16).

4.3 Choice of hyperparameters

The hyperparameters of the *feature extractor* (e.g. kernel sizes, filters) are adopted from [55]. A similar extractor with the same hyperparameters has been used in several multimodal emotion recognition tasks with state-of-the-art performance [13], [55].

As the *prior distribution* $P(w)$, [23] recommend a mixture of two Gaussians, with zero means and standard deviations as $\sigma_1 > \sigma_2$ and $\sigma_2 \ll 1$, thereby obtaining a spike-and-slab prior with heavy tail and concentration around zero mean. But in our case, we do not need mean centered predictions, as \mathcal{Y} does not follow such a distribution in both datasets (see Sec. 4.1). In this light, we propose to use a simple Gaussian prior with unit standard deviation $\mathcal{N}(0, 1)$. Moreover, a simple $\mathcal{N}(0, 1)$ prior initialization also makes the proposed model scalable across SER datasets.

TABLE 1: Comparison on mean m , standard deviation s , and label distribution estimations \mathcal{Y} , in terms of $\mathcal{L}_{ccc}(m)$, $\mathcal{L}_{ccc}(s)$, and \mathcal{L}_{KL} , respectively. Larger CCC indicates improved performance as indicated by \uparrow . Lower KL indicates improved performance as indicated by \downarrow . ** indicates that the respective approach achieves statistically significant better results than *all* other approaches in comparison. * indicates that it achieves statistically significant better results over *only some* of the approaches in comparison. Results in brackets (.) are for the respective development partition of the dataset.

	Arousal			Valence		
	$\mathcal{L}_{ccc}(m) \uparrow$	$\mathcal{L}_{ccc}(s) \uparrow$	$\mathcal{L}_{KL} \downarrow$	$\mathcal{L}_{ccc}(m) \uparrow$	$\mathcal{L}_{ccc}(s) \uparrow$	$\mathcal{L}_{KL} \downarrow$
E2E Baseline	0.7609	-	-	0.3529	-	-
STL [9]	0.7192	-	-	0.3878	-	-
MTL PU [9]	0.7336	0.2861	0.7965	0.4163**	0.0292	0.9981
MU [38]	0.7559	0.0764	0.6900	0.3248	0.0359	0.6334
MU+LU [38]	0.7437	0.3402	0.2576	0.2831	0.0422	0.4054
<i>t</i>-LU (proposed)	0.7665*	0.3752**	0.2349**	0.3768*	0.0481*	0.3914*

(a) Quantitative results on AVEC'16 dataset.

	Arousal			Valence		
	$\mathcal{L}_{ccc}(m) \uparrow$	$\mathcal{L}_{ccc}(s) \uparrow$	$\mathcal{L}_{KL} \downarrow$	$\mathcal{L}_{ccc}(m) \uparrow$	$\mathcal{L}_{ccc}(s) \uparrow$	$\mathcal{L}_{KL} \downarrow$
E2E Baseline	0.3697 (0.4041)	-	-	0.1919 (0.1827)	-	-
STL [9]	0.2912 (0.3591)	-	-	0.1902 (0.1887)	-	-
MTL PU [9]	0.2956 (0.3624)	0.1066 (0.1051)	0.5288 (0.4415)	0.1811 (0.1847)	0.0295 (0.0292)	0.5608 (0.4515)
MU [38]	0.3668 (0.4064)	0.0516 (0.0668)	0.3802 (0.4098)	0.2075 (0.2201)	0.0216 (0.0276)	0.4513 (0.4389)
MU+LU [38]	0.3552 (0.3951)	0.1104 (0.1211)	0.3690 (0.3215)	0.1894 (0.2165)	0.0287 (0.0311)	0.4111 (0.3976)
<i>t</i>-LU (proposed)	0.3889** (0.4211**)	0.1181* (0.1338*)	0.3571** (0.3169**)	0.2117** (0.2226**)	0.0306* (0.0340*)	0.3734** (0.3837**)

(b) Quantitative results on MSPConv dataset.

The μ_w and ρ_w of the *posterior distribution* $P(w|D)$ are initialized uniformly in the range $[-0.1, 0.1]$ and $[-3, -2]$, respectively. The ranges were fine-tuned using grid search for maximized \mathcal{L}_{KL} . For AVEC'16, as the test partition is not publicly available, fine-tuning is performed on the train partition. For MSPConv, the development partition is used.

It is computationally expensive to sample new weights at every time-step (40 ms) and also the level of uncertainties varies rather slowly. In this light, for the AVEC'16 dataset, we set the *BBB window-size* $b = 2$ s (50 frames). As the MSPConv dataset is comparatively larger, a compromise was made for computational simplicity and $b = 4$ s (100 frames) is used. For median filtering, the sole post-processing technique used, a window-size of 2 s is used.

In this work, we assume a Gaussian on $\hat{\mathcal{Y}}_t$, and noted previously that $n \geq 30$ is required for the assumption to hold. In this light, and keeping the time-complexity in mind, we fixed $n = 30$. For training, we use the Adam optimizer with learning rate 10^{-4} . The batch size used was 5, with a sequence length of 300 frames, 40 ms each. All models were trained for a fixed 100 epochs.

4.4 Validation measures

To validate the proposed method's *mean* and *standard deviation* estimates, we use $\mathcal{L}_{CCC}(m)$ and $\mathcal{L}_{CCC}(s)$ metrics, respectively, widely used in literature [9], [11], [55]. However, $\mathcal{L}_{CCC}(m)$ and $\mathcal{L}_{CCC}(s)$ validate mean and standard deviation estimates *separately*. To further jointly validate mean and standard deviation estimates, as label distribution $\hat{\mathcal{Y}}_t$, we use the \mathcal{L}_{KL} measure. For a fair comparison, we validate all the models in comparison using \mathcal{L}_{KL} based on their respective distribution assumptions on \mathcal{Y}_t , as the models are trained in a similar fashion. The proposed *t-LU* version is validated and trained on the *t*-distribution \mathcal{L}_{KL} (16), and the

baselines on the Gaussian \mathcal{L}_{KL} (12). Nevertheless, from the experiments, we also noted that the proposed *t-LU* performs better in-terms of both (16) and (12).

5 RESULTS AND DISCUSSION

5.1 Quantitative analysis of estimates

Table 1 shows the average performance of the baselines and the proposed models, in terms of their mean m , standard deviation s , and distribution $\hat{\mathcal{Y}}_t$ estimations, $\mathcal{L}_{CCC}(m)$, $\mathcal{L}_{CCC}(s)$ and \mathcal{L}_{KL} , respectively. Results for AVEC'16 are seen in Table 1a, and for MSPConv in Table 1b. Statistical significance is estimated using one-tailed *t*-test, asserting significance for p -values ≤ 0.05 , similar to [5].

5.1.1 Comparison on mean estimates

In terms of mean estimates $\mathcal{L}_{CCC}(m)$ of *arousal*, Table 1 shows that the proposed *t-LU* model performs *best* in comparison with the baselines, in both AVEC'16 (Table 1a) and MSPConv (Table 1b) datasets, with *statistical significance*. The improved $\mathcal{L}_{CCC}(m)$ estimates are however not statistically significant over the E2E Baseline in AVEC'16. Three key takeaways can be noted from the $\mathcal{L}_{CCC}(m)$ results for *arousal*. Firstly, it is noted that the BBB-LDL baselines (MU, MU+LU, and *t-LU*) achieve better $\mathcal{L}_{CCC}(m)$ than the MTL baselines (STL, and MTL PU). In case of the more complex MSPConv dataset the better performance is more evident, where *t-LU* improves over E2E Baseline by 0.006 and 0.019 $\mathcal{L}_{CCC}(m)$ in AVEC'16 and MSPConv, respectively. Secondly, between the BBB-LDL versions, the superiority of the proposed *t*-distribution \mathcal{L}_{KL} (16) over the Gaussian \mathcal{L}_{KL} (12) is noted, with *t-LU* outperforming MU+LU in both the dataset. Thirdly, while including uncertainty modeling in the E2E Baseline, a *compromise* on $\mathcal{L}_{CCC}(m)$ is made with improving uncertainty estimates ($\mathcal{L}_{CCC}(s)$ and \mathcal{L}_{KL}), seen

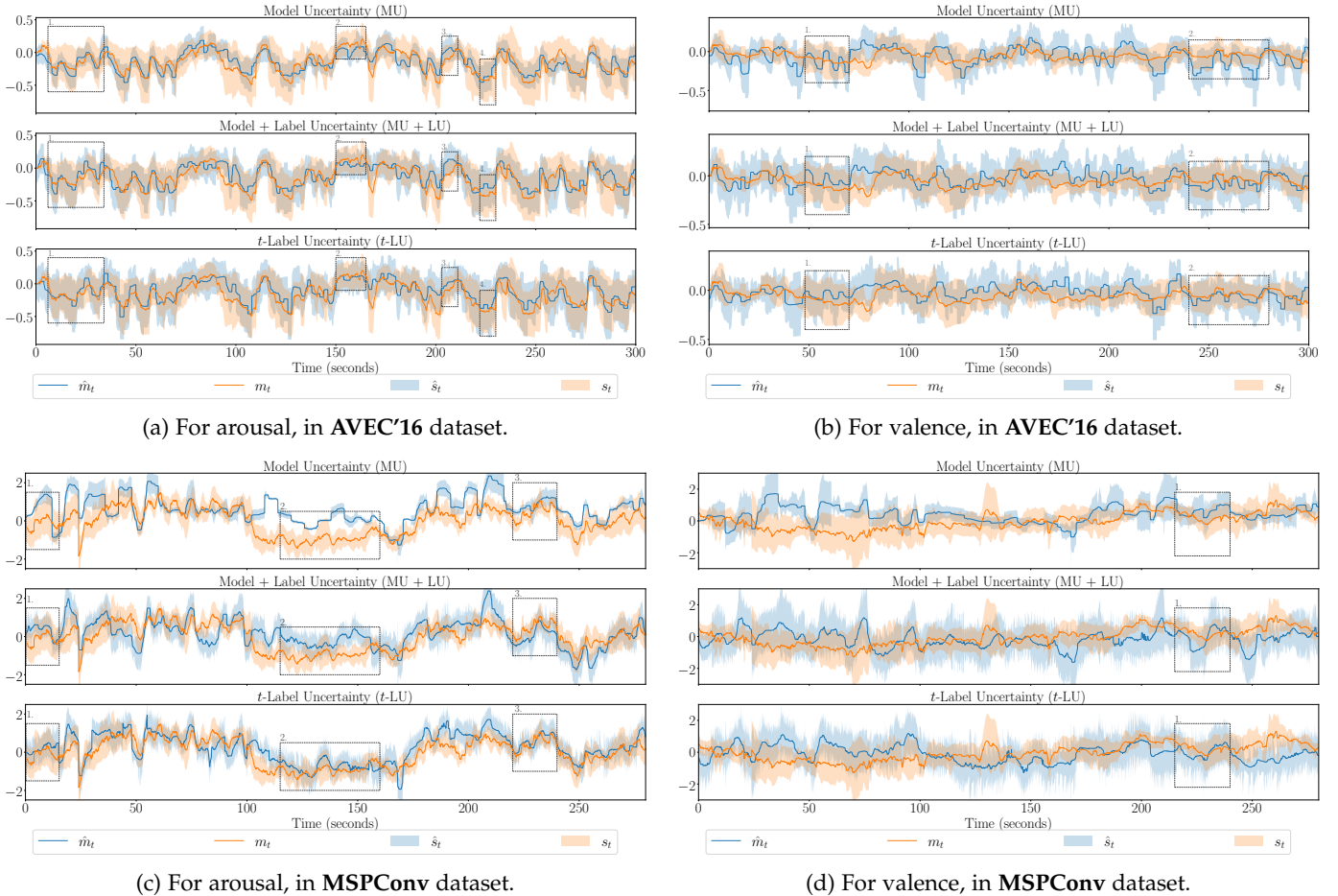


Fig. 5: Label distribution \mathcal{Y}_t estimation results for a test subject.

when comparing MU and MU+LU results with that of E2E Baseline. However, the proposed t -LU is free from this compromise, outperforming the E2E Baseline and other BBB-LDL versions. In the test partitions, the t -LU achieves $\mathcal{L}_{CCC}(m)$ of 0.7665 in AVEC'16 and 0.3889 in MSPConv, with E2E Baseline achieving 0.7609 and 0.3797, respectively.

In terms of mean estimates $\mathcal{L}_{CCC}(m)$ of *valence*, in AVEC'16, the MTL based uncertainty baseline, MTL PU, performs significantly better than all other models in comparison. However, in the larger and more complex MSPConv dataset, the proposed t -LU performs best, with statistical significance. Similar to arousal, for valence, we see that t -LU is free from compromises on $\mathcal{L}_{CCC}(m)$ with improving uncertainty estimates, with t -LU significantly outperforming the E2E baseline. In the test partitions, the t -LU achieves $\mathcal{L}_{CCC}(m)$ of 0.3768 in AVEC'16 and 0.2117 in MSPConv, with the E2E Baseline achieving 0.3529 and 0.1919, respectively. It can also be noted that, all the proposed models and the baselines, generally show reduced performance in the MSPConv dataset, when compared to AVEC'16. This can be owed to the complexity of the dataset along with the noisy annotations of the dataset (see Sec. 4.1). However, the general trends in model comparisons still exists.

5.1.2 Comparison on uncertainty estimates

Concerning the uncertainty estimates in *arousal*, Table 1 shows that the proposed t -LU achieves state-of-the-art re-

sults, in terms of both $\mathcal{L}_{CCC}(s)$ and \mathcal{L}_{KL} . In AVEC'16, the improvements are always accompanied by statistical significance. But, in MSPConv, on the one hand, in terms of $\mathcal{L}_{CCC}(s)$, statistical significance does not exist when compared with MU+LU, however exists with all other baselines. On the other hand, in terms of \mathcal{L}_{KL} , the improvements by t -LU are statistically significant over all baselines. For instance, in AVEC'16, t -LU achieves 0.3752 $\mathcal{L}_{CCC}(s)$ and 0.2349 \mathcal{L}_{KL} , improving with statistical significance. In MSPConv, t -LU achieves 0.1181 $\mathcal{L}_{CCC}(s)$ and 0.3571 \mathcal{L}_{KL} , where statistical significance over *all* other baselines exists only for \mathcal{L}_{KL} . Reasons for this trend is that, firstly, the MSPConv is more complex with larger levels of subjectivity (see Sec. 4.1). Secondly, the model is exclusively trained on \mathcal{L}_{KL} , so direct improvements over \mathcal{L}_{KL} is expected rather on $\mathcal{L}_{CCC}(s)$.

For *valence*, in AVEC'16, unlike the $\mathcal{L}_{CCC}(m)$ performances, Table 1a shows that the proposed t -LU achieves improved performance in terms of the *uncertainty estimates*, over all the baselines in comparison. It is further noted that t -LU improves with statistical significance over the MTL-based baselines, however improves without statistical significance in comparison with the BBB-based baselines. While the MU+LU achieves a $\mathcal{L}_{CCC}(s)$ and \mathcal{L}_{KL} of 0.0422 and 0.405, respectively, the proposed t -LU improves by achieving 0.0481 and 0.3914, respectively. In MSPConv, seen in Table 1b, the proposed t -LU achieves state-of-the-art uncertainty estimates in terms of both measures. Similar

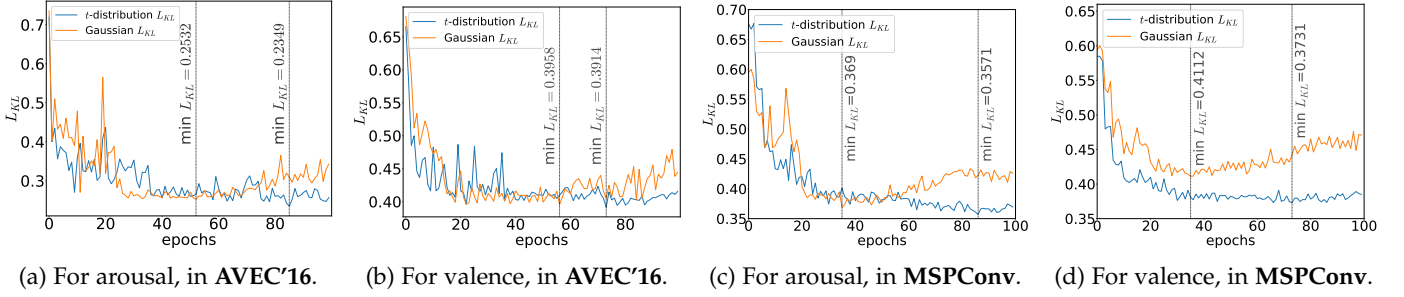


Fig. 6: Loss curve comparison between Gaussian \mathcal{L}_{KL} (12) and proposed t -distribution \mathcal{L}_{KL} (16).

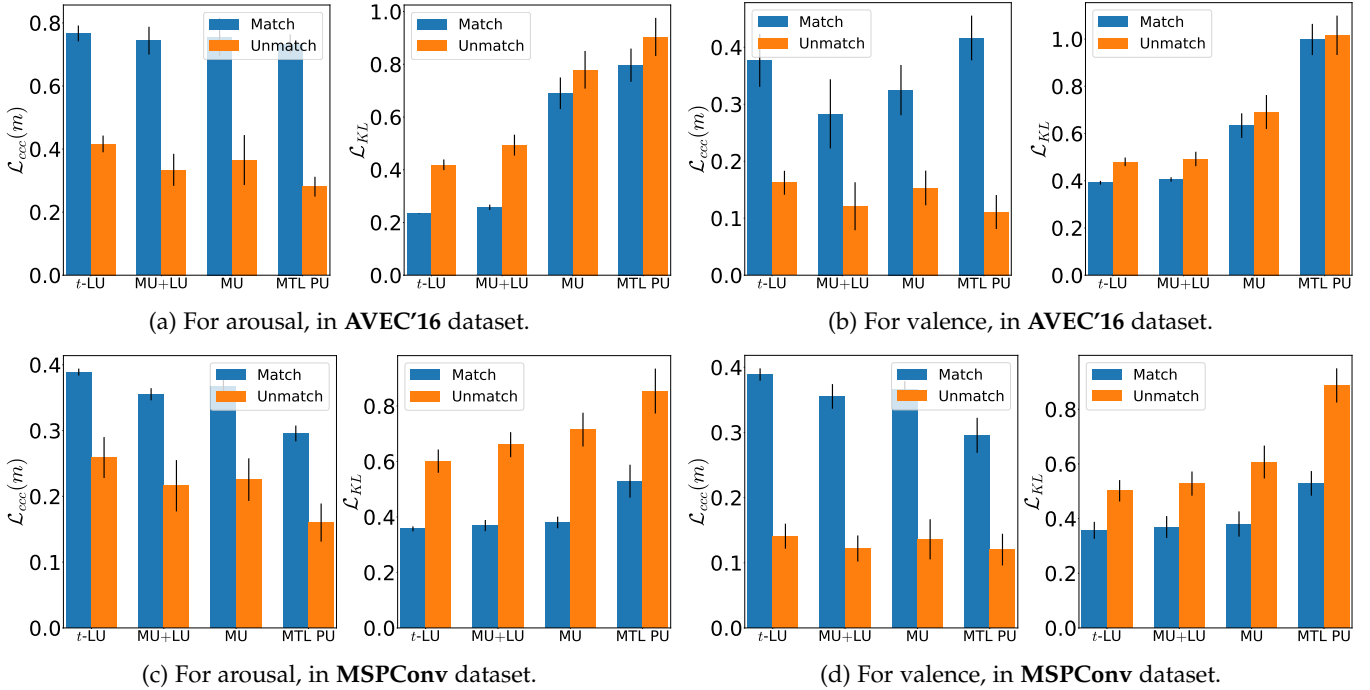


Fig. 7: Cross-corpora evaluations, for Match and Unmatch conditions in terms of $\mathcal{L}_{ccc}(m)$ and \mathcal{L}_{KL} .

to arousal, statistical significance exists over *all* baselines for \mathcal{L}_{KL} , and over *only some* of the baselines for $\mathcal{L}_{CCC}(s)$. These superior results achieved by t -LU explains the advantage of using the t -distribution based \mathcal{L}_{KL} loss (16) for label uncertainty modeling. The t -distribution \mathcal{L}_{KL} is mathematically more sound, and as seen in Figure 2 promotes the model to fit on a more relaxed s_t and penalizes more for tighter standard deviations, thereby leading to better capturing the label distribution.

5.2 Qualitative analysis of estimates

For qualitative analyses, we plot the mean \hat{m}_t and standard deviation \hat{s}_t estimates of $\hat{\mathcal{Y}}_t$ against the m_t and standard deviation s_t of ground-truth distribution \mathcal{Y}_t . Plots for a test subject from AVEC'16, in terms of arousal and valence, can be seen in figures 5a and 5b, respectively, and, for MSPConv, in figures 5c and 5d, respectively. Parts of the plots are boxed and numbered to note performance differences.

For *arousal*, in figures 5a and 5c, further backing the results in Table 1, the proposed t -LU model best captures m and s of the annotation distribution \mathcal{Y}_t , in comparison with MU and MU+LU. For example, in AVEC'16 (see Fig. 5a),

in box 2, the proposed t -LU captures the whole annotation distribution \mathcal{Y}_t , where \hat{s}_t best resembles s_t . This further highlights the robustness of training on a relaxed σ_t through a t -distribution. Similarly, in MSPConv (see Fig. 5c), from boxes 2 and 3, the proposed t -LU by best capturing s , and also improves notably in terms of the mean estimates m . However, the resemblance of \hat{s}_t to s_t is more perfect for AVEC'16, than the more complex MSPConv. At the same time, the improvements made by t -LU are more evident on MSPConv than on AVEC'16, backing the results of statistical significance tests presented in Table 1b.

For *valence*, from figures 5b and 5d, on both datasets, the proposed t -LU evidently improves on mean estimates m_t , with only small improvements on standard deviation estimates s . This can be seen for instance in box 1 (see Fig. 5b), where t -LU, in comparison with MU and MU+LU, notably improves on m_t , while only small improvements can be noted on s_t . This reveals that capturing s_t in valence by only relying on audio is a challenging task. It is a common trend in literature that the audio modality insufficiently explains ground-truth valence m_t [13], [58], and this trend is even more challenging for modeling s_t in valence.

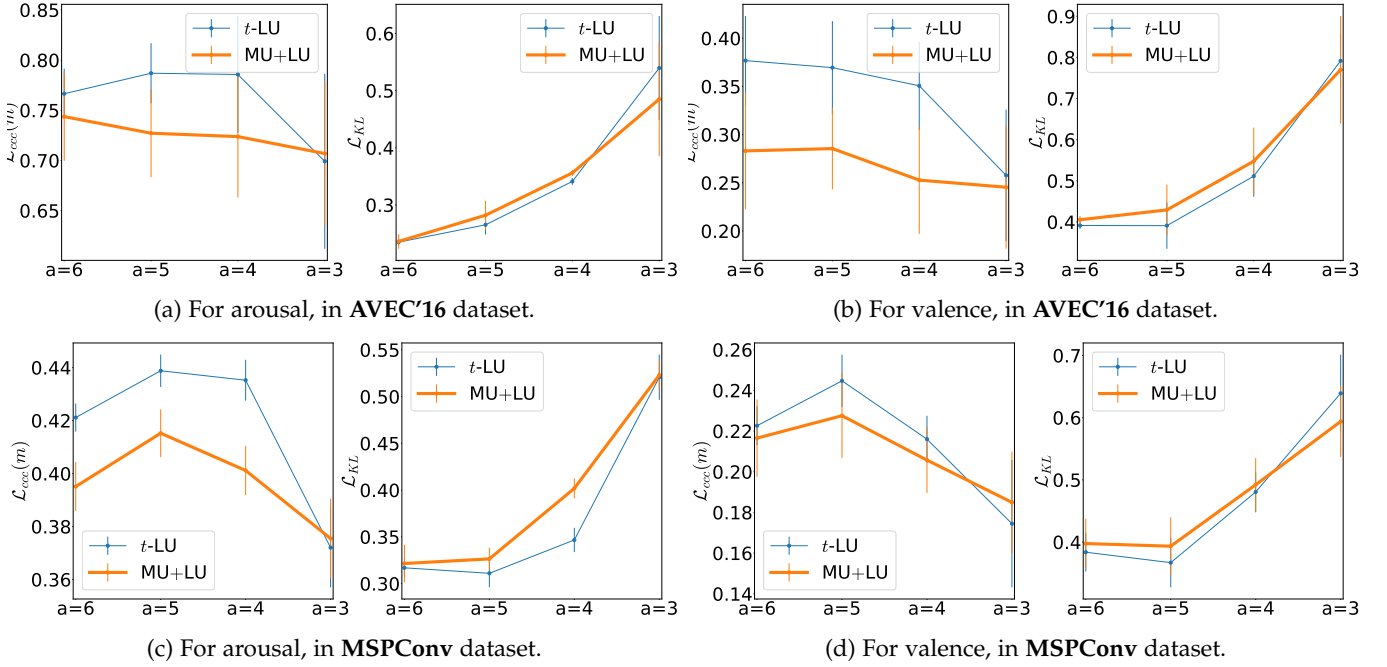


Fig. 8: Impact of number of annotations available $a = 6, 5, 4, 3$ on $\mathcal{L}_{\text{ccc}(m)}$ and \mathcal{L}_{KL} .

5.3 Analysis on training loss curve

To further study the advantages of the proposed t -distribution \mathcal{L}_{KL} (16) during the training phase, we compare the testing loss curve of (16) with the Gaussian \mathcal{L}_{KL} in MU+LU (12). The comparisons can be seen in Figure 6.

In both the datasets, Figure 6 illustrates two crucial advantages of the proposed t -distribution \mathcal{L}_{KL} loss term (16) during training. Firstly, we see that in the initial epochs, before epoch 20, the proposed loss converges quicker than the Gaussian \mathcal{L}_{KL} (12). This is the result of the proposed \mathcal{L}_{KL} (16) loss term which penalizes more for lower s_t values, in comparison to the Gaussian \mathcal{L}_{KL} (12) (see Sec. 3.3.3), thereby achieving faster convergence. Secondly, it is noted that during the later epochs, after epoch 70, the Gaussian \mathcal{L}_{KL} (12) shows signs of overfitting, which is more evident in the MSPConv dataset. However, at the same time, the proposed t -distribution \mathcal{L}_{KL} (16) converges to the best minima during the later epochs. For instance, in MSPConv, the proposed (16) achieves minima \mathcal{L}_{KL} at epoch 86, with \mathcal{L}_{KL} of 0.3571 for arousal and 0.3734 for valence, while the Gaussian achieves a minima well before the later epochs, at epoch 35, with \mathcal{L}_{KL} of 0.3690 for arousal and 0.4112 for valence. The proposed \mathcal{L}_{KL} (16) is free from overfitting in the later stages of training and also learns the optima at this stage, noticed across two datasets. This behaviour can be attributed to the nature of the proposed \mathcal{L}_{KL} (16) which promotes the model to learn a more relaxed s_t , thereby introducing more regularization to the model, preventing overfitting and converging on an improved s_t .

5.4 Cross-corpora evaluation

We performed cross-corpora evaluations using AVEC'16 and MSPConv datasets. Results are presented in terms of $\mathcal{L}_{\text{ccc}(m)}$ and \mathcal{L}_{KL} , under two conditions, in Figure 7. The *Match* condition where the train and the test partitions come

from the *same* dataset, and the *Unmatch* condition where the *train* partition is from a *different* dataset. Apart from the size of the datasets, dataset-specific factors, such as population demographics and social context, severely challenge the cross-corpora performances. Crucial differences exist between the two datasets used in this paper. While the social context of AVEC'16 is a *dyadic* interaction in a *virtual* setting, MSPConv comprises of *larger groups* in a *face-to-face* setting. Literature indicates human behaviour varies across group-sizes [36] and social contexts [32]. Moreover, AVEC'16 was collected from *french-speaking* subjects, while MSPConv from *english-speaking* ones.

In comparison with the uncertainty baselines, the proposed t -LU achieves the best performance in the cross-corpora evaluation on both datasets. Under the *Unmatch* condition, for *arousal* in AVEC'16 (see Fig. 7a), t -LU achieves 0.4163 $\mathcal{L}_{\text{ccc}(m)}$ and 0.4188 \mathcal{L}_{KL} , while MU achieves 0.3342 and 0.4934, respectively. Similarly, in MSPConv (see Fig. 7c), t -LU achieves 0.2590 $\mathcal{L}_{\text{ccc}(m)}$ and 0.6011 \mathcal{L}_{KL} , while MU achieves 0.2161 and 0.6605, respectively. All models in comparison show performance degrade from the *Match* to *Unmatch* conditions. In terms of $\mathcal{L}_{\text{ccc}(m)}$, for both arousal and valence, t -LU achieves the *least degrade percentage* while the MTL PU results in the *highest* degrade. For instance, in AVEC'16, in terms of *arousal* mean-estimates $\mathcal{L}_{\text{ccc}(m)}$ (see Fig. 7a), t -LU achieves the least degradation of 46% and MTL PU degrades the most with 62%. Similarly, for *valence* (see Fig. 7b), t -LU degrades least with 56%, and MTL PU degrades the most with 63%. Unlike the proposed t -LU, the MTL PU requires a dataset-dependent tuning of loss function, thereby resulting in maximum degradation. The *degrade percentage* in \mathcal{L}_{KL} is not comparable as the scale of the measure is not linear (depicted in Fig. 2). Also notable is that, for all models, the *degrade percentage* is larger for valence than for arousal.

TABLE 2: Ablation study results of the t -LU model, on the AVEC'16 [37] and MSP-Conversation [31] datasets. Modules included in the ablation study are the Uncertainty Layer (BBB), the end-to-end Feature Extractor (E2E), and the Label Distribution Learning loss (KL). \checkmark denotes the *inclusion* of the respective module, and \times its *omission*. **Bold** results denote the *best two* results for a particular metric, and underline denotes the *least two*.

	Modules			Arousal			Valence		
	E2E	BBB	KL	$\mathcal{L}_{\text{ccc}}(m) \uparrow$	$\mathcal{L}_{\text{ccc}}(s) \uparrow$	$\mathcal{L}_{\text{KL}} \downarrow$	$\mathcal{L}_{\text{ccc}}(m) \uparrow$	$\mathcal{L}_{\text{ccc}}(s) \uparrow$	$\mathcal{L}_{\text{KL}} \downarrow$
AVEC'16	\checkmark	\checkmark	\checkmark	0.7665	0.3752	0.2349	0.3768	0.0481	0.3914
	\checkmark	\checkmark	\times	0.7392	0.3507	0.4133	<u>0.3109</u>	0.0522	0.5961
	\checkmark	\times	\checkmark	<u>0.6970</u>	<u>0.3107</u>	0.2962	0.3721	0.0390	0.4257
	\checkmark	\times	\times	0.7189	0.3910	<u>0.5111</u>	0.3961	0.0634	<u>0.8628</u>
	\times	\checkmark	\checkmark	0.7640	<u>0.2866</u>	0.2772	0.3599	<u>0.0327</u>	0.4143
	\times	\checkmark	\times	0.7457	0.3278	0.4463	<u>0.3251</u>	0.0493	0.6016
	\times	\times	\checkmark	<u>0.7151</u>	0.3265	0.3190	0.3772	<u>0.0388</u>	0.4470
	\times	\times	\times	0.7336	0.2861	<u>0.7965</u>	0.4163	0.0292	<u>0.9981</u>
MSPConv	\checkmark	\checkmark	\checkmark	0.3889	0.1181	0.3571	0.2117	0.0306	0.3734
	\checkmark	\checkmark	\times	0.2847	0.0958	0.4136	0.1790	0.0293	0.4960
	\checkmark	\times	\checkmark	<u>0.1624</u>	<u>0.0502</u>	0.5192	<u>0.1206</u>	<u>0.0091</u>	0.5371
	\checkmark	\times	\times	0.2707	0.1001	0.4893	0.1736	0.0115	<u>0.5933</u>
	\times	\checkmark	\checkmark	0.4002	0.0559	0.3920	0.2300	0.0169	0.3988
	\times	\checkmark	\times	0.3074	0.0783	<u>0.5518</u>	0.1804	0.0206	0.4162
	\times	\times	\checkmark	<u>0.2460</u>	<u>0.0396</u>	0.4972	<u>0.1397</u>	<u>0.0052</u>	0.5799
	\times	\times	\times	0.2956	0.1066	<u>0.5288</u>	0.1811	0.0295	<u>0.5908</u>

5.5 Impact of number of annotations a available

In Sec. 5.1, we noted the benefits of modeling \mathcal{Y}_t as a t -distribution, with *six* available annotations ($a = 6, \nu = 6$). To emphasize on the benefits of the t -distribution t -LU over the Gaussian MU+LU, especially when *fewer annotations* are available, we performed experiments by varying a and thereby the degrees of freedom ν . The results are presented in Figure 8, under 4 settings, $a = 3, a = 4, a = 5$, and $a = 6$. The order of annotation to be ignored for the experiment is handled based on the Pearson’s correlations measure, with the least correlating annotation ignored first for a sample.

From Figure 8, *especially when $n \geq 4$* , it is noted that the t -distribution based t -LU shows superior performance over the Gaussian MU+LU, on both datasets. Crucially, the improvements are larger and more evident when $a = 4$ and $a = 5$, than when $a = 6$. As annotations are ignored in the order of correlation, this reveals that the advantage of t -distribution over the Gaussian grows with increasing inter-annotator correlation and reducing number of available annotations. However, both the t -LU and MU+LU suffer when only 3 annotations are available ($a = 3$), as a stable distribution \mathcal{Y}_t cannot be modeled with only 3 samples. Moreover, when $a = 3$, performance of t -LU drop below that of Gaussian MU+LU. This is due to the fact that t -LU model becomes highly uncertainty with only 3 annotations, because of the large relaxation on s_t introduced by the scaling in Equation 7. This behaviour is similar to the t -test calculation, where models become more uncertain with reducing ν . We therefore recommend the t -distribution when more than 3 annotations are available. Noting that the Gaussian also performs equally bad with only 3 annotations, we suggest collecting at least 4 annotations to obtain a reliable annotation distribution and its ground-truth consensus.

5.6 Ablation study

The proposed end-to-end label uncertainty model has three crucial modules (see Fig. 1), namely 1) feature extractor, 2) uncertainty layer, and, 3) label uncertainty loss. To understand the modules’ specific contributions, we perform an

ablation study, whose results are presented in Table 2. In case of the feature extractor, $E2E$, \checkmark denotes usage of an end-to-end feature extractor and \times the hand-crafted features [20], [59]. In case of the uncertainty layer, BBB , \checkmark denotes usage of the BBB-based uncertainty layer and \times the MTL-based σ_t uncertainty estimator. For label uncertainty loss, KL , \checkmark denotes using \mathcal{L}_{KL} loss and \times denotes usage of $\mathcal{L}_{\text{ccc}}(s)$ loss.

From Table 2, firstly, it is noted that end-to-end models achieve better uncertainty estimates than hand-crafted feature models. For instance, in AVEC'16, $E2E$ based BBB - KL model achieves 0.3752 $\mathcal{L}_{\text{ccc}}(s)$ and 0.2349 \mathcal{L}_{KL} , improving over hand-crafted features based BBB - KL model, which achieves 0.2866 and 0.2772, respectively. Similarly, in the larger and more complex MSPConv, the $E2E$ based BBB - KL model achieves the best uncertainty estimate performances, against all other models in comparison, with 0.1181 $\mathcal{L}_{\text{ccc}}(s)$ and 0.3571 \mathcal{L}_{KL} . This trend is inline with literature which suggest end-to-end learning for uncertainty modeling [14].

Secondly, it is observed that the combination of BBB -based uncertainty layer and KL -based loss term results in improved performances in both mean and uncertainty estimates, suggesting the combination of BBB -layer and KL -loss for label uncertainty modeling in SER. The performance of BBB -layer with a $\mathcal{L}_{\text{ccc}}(s)$ loss term degrades performance across metrics. An intuition behind this trend is that KL -based *distribution* loss is apt for optimizing the weight *distributions* $P(w|\mathcal{D})$, rather than a loss with only optimizes for s_t of label distribution. Thirdly, in both datasets, the KL -based loss term contributes to the improvement of both uncertainty and mean estimates, as the KL loss jointly optimizes m_t and s_t estimates. For instance, using the KL loss in the $E2E$ - BBB architecture results in an $\mathcal{L}_{\text{ccc}}(m)$ improvement of 3% in AVEC'16 and 35% in MSPConv. Similarly, in-terms of $\mathcal{L}_{\text{ccc}}(m)$, improvements of 9% and 23% are noted, in AVEC'16 and MSPConv, respectively. Finally, it is noted that the MTL-based uncertainty models collapse when not trained on $\mathcal{L}_{\text{ccc}}(s)$ loss, and are not capable of distribution learning using the \mathcal{L}_{KL} loss. However, though BBB -based

models perform best when trained on \mathcal{L}_{KL} , they produce competitive results with both \mathcal{L}_{KL} and $\mathcal{L}_{\text{cc}}(s)$. Overall, these trends suggest that BBB-based \mathcal{Y}_t learning models outperform MTL-based s_t estimating models in estimating label uncertainty in SER.

6 CONCLUSION

We introduced an end-to-end BNN capable of modeling emotion annotations as a label distribution, thereby accounting for the inherent subjectivity-based label uncertainty. In the literature, emotion annotations are commonly modeled using a Gaussian or a histogram distribution, however with only limited annotations. In contrast, in this work, we modeled ground-truth emotion annotations as a Student's t -distribution, which also accounts for the number of annotations available. For this, we derived a t -distribution based KL divergence loss that, for limited annotations, is mathematically more sound. We showed that the proposed t -distribution loss term leads to training on a relaxed standard deviation, which is adaptable with respect to the number of annotations available. We validated our approach on two publicly available in-the-wild datasets. Quantitative analysis of the results showed that the proposed approach achieves state-of-the-art results in mean and uncertainty estimations, in-terms of both CCC and KL divergence measures, which were also consistent for cross-corpora evaluations. By analysing the loss curves, we showed that the proposed loss term leads to faster and improved convergence, and is less prone to overfitting. It was also revealed that the advantage of t -distribution over the Gaussian grows with increasing inter-annotator correlation and reducing number of available annotations. Trends noted in the ablation study suggested that, for label uncertainty modeling in SER, BBB-based label distribution learning models are to be preferred over estimating standard-deviation as an auxiliary task.

REFERENCES

- [1] G. A. Van Kleef, "How emotions regulate social life: The emotions as social information (easi) model," *Current directions in psychological science*, vol. 18, no. 3, pp. 184–188, 2009.
- [2] B. W. Schuller, "Speech emotion recognition: two decades in a nutshell, benchmarks, and ongoing trends," *Communications of the ACM*, vol. 61, no. 5, pp. 90–99, Apr. 2018.
- [3] J. A. Russell, "A circumplex model of affect," *Journal of personality and social psychology*, vol. 39, no. 6, p. 1161, 1980.
- [4] D. Dukes, K. Abrams, R. Adolphs, M. E. Ahmed, A. Beatty, K. C. Berridge, S. Broomhall, T. Brosch, J. J. Campos, Z. Clay *et al.*, "The rise of affectivism," *Nature Human Behaviour*, pp. 1–5, 2021.
- [5] K. Sridhar, W.-C. Lin, and C. Busso, "Generative approach using soft-labels to learn uncertainty in predicting emotional attributes," in *IEEE Int. Conf. on Affective Computing and Intelligent Interaction*, Virtual Event, Oct. 2021, pp. 1–8.
- [6] C. Busso, M. Bulut, C.-C. Lee, A. Kazemzadeh, E. Mower, S. Kim, J. N. Chang, S. Lee, and S. S. Narayanan, "Iemocap: Interactive emotional dyadic motion capture database," *Language resources and evaluation*, vol. 42, no. 4, pp. 335–359, 2008.
- [7] M. Grimm and K. Kroschel, "Evaluation of natural emotions using self assessment manikins," in *IEEE Workshop on Automatic Speech Recognition and Understanding*, Jan. 2005, pp. 381–385.
- [8] H. Gunes and B. Schuller, "Categorical and dimensional affect analysis in continuous input: Current trends and future directions," *Image and Vision Computing*, vol. 31, pp. 120–136, 2013.
- [9] J. Han, Z. Zhang, Z. Ren, and B. Schuller, "Exploring perception uncertainty for emotion recognition in dyadic conversation and music listening," *Cognitive Computation*, vol. 13, Mar. 2021.
- [10] K. Sridhar and C. Busso, "Modeling uncertainty in predicting emotional attributes from spontaneous speech," in *IEEE Int. Conf. on Acoustics, Speech, Sig. Proc., ICASSP*, Barcelona, Spain, May 2020.
- [11] P. Tzirakis, J. Zhang, and B. W. Schuller, "End-to-End Speech Emotion Recognition Using Deep Neural Networks," in *IEEE Int. Conf. on Acoustics, Speech, Sig. Proc., ICASSP*, Calgary, Canada, Apr. 2018.
- [12] J. Huang, Y. Li, J. Tao, Z. Lian, and J. Yi, "End-to-end continuous emotion recognition from video using 3D ConvLSTM networks," in *IEEE Int. Conf. on Acoustics, Speech, Sig. Proc., ICASSP*, Apr. 2018.
- [13] P. Tzirakis, J. Chen, S. Zafeiriou, and B. Schuller, "End-to-end multimodal affect recognition in real-world environments," *Information Fusion*, vol. 68, pp. 46–53, 2021.
- [14] S. Alisamir and F. Ringeval, "On the evolution of speech representations for affective computing: A brief history and critical overview," *IEEE Signal Proc., Magazine*, vol. 38, pp. 12–21, 2021.
- [15] A. Kendall and Y. Gal, "What uncertainties do we need in Bayesian deep learning for computer vision?" in *Advances in Neural Inf. Proc. Sys., NeurIPS*, vol. 30, Dec. 2017.
- [16] R. Zheng, S. Zhang, L. Liu, Y. Luo, and M. Sun, "Uncertainty in Bayesian deep label distribution learning," *Applied Soft Computing*, vol. 101, Mar. 2021.
- [17] M. K. Tellamekala, T. Giesbrecht, and M. Valstar, "Dimensional affect uncertainty modelling for apparent personality recognition," *IEEE Tran. on Affective Computing*, Jul. 2022.
- [18] J. Liu, J. Paisley, M.-A. Kioumourtoglou, and B. Coull, "Accurate uncertainty estimation and decomposition in ensemble learning," in *Advances in Neural Inf. Proc. Sys., NeurIPS*, Vancouver, Dec. 2019.
- [19] S. Kohl, B. Romera-Paredes, C. Meyer, J. De Fauw, J. R. Ledsam, K. Maier-Hein, S. Eslami, D. Jimenez Rezende, and O. Ronneberger, "A probabilistic U-Net for segmentation of ambiguous images," in *Advances in Neural Inf. Proc. Sys., NeurIPS*, Montreal, Canada, Dec. 2018.
- [20] M. K. Tellamekala, E. Sanchez, G. Tzimiropoulos, T. Giesbrecht, and M. Valstar, "Stochastic Process Regression for Cross-Cultural Speech Emotion Recognition," in *Interspeech*, Brno, Sep. 2021.
- [21] M. Garnelo, D. Rosenbaum, C. Maddison, T. Ramalho, D. Saxton, M. Shanahan, Y. W. Teh, D. Rezende, and S. A. Eslami, "Conditional neural processes," in *Int. Conf. Machine Learning (ICML)*, Stockholm, Sweden, Jul. 2018.
- [22] Y. Gal and Z. Ghahramani, "Dropout as a Bayesian approximation: Representing model uncertainty in deep learning," in *Int. Conf. Machine Learning (ICML)*, New York City, NY, USA, Jun. 2016.
- [23] C. Blundell, J. Cornebise, K. Kavukcuoglu, and D. Wierstra, "Weight uncertainty in neural network," in *Int. Conf. Machine Learning (ICML)*, Lille, France, Jul. 2015.
- [24] H. Fang, T. Peer, S. Wermter, and T. Gerkmann, "Integrating statistical uncertainty into neural network-based speech enhancement," in *IEEE Int. Conf. on Acoustics, Speech, Sig. Proc., ICASSP*, Singapore, Jan. 2022.
- [25] B.-B. Gao, C. Xing, C.-W. Xie, J. Wu, and X. Geng, "Deep label distribution learning with label ambiguity," *IEEE Transactions on Image Processing*, vol. 26, no. 6, pp. 2825–2838, 2017.
- [26] N. M. Foteinopoulou, C. Tzelepis, and I. Patras, "Estimating continuous affect with label uncertainty," in *IEEE Int. Conf. on Affective Computing and Intelligent Interaction*, Virtual Event, Oct. 2021.
- [27] S. Kotz and S. Nadarajah, *Multivariate t-distributions and their applications*. Cambridge University Press, 2004.
- [28] C. M. Bishop and N. M. Nasrabadi, *Pattern Recognition and Machine Learning*, Berlin, Heidelberg. Springer, 2006.
- [29] C. Villa and F. J. Rubio, "Objective priors for the number of degrees of freedom of a multivariate t distribution and the t-copula," *Computational Statistics & Data Analysis*, vol. 124, pp. 197–219, 2018.
- [30] H. Fischer, *A History of the Central Limit Theorem: From Classical to Modern Probability Theory*. Springer New York, 2010.
- [31] L. Martinez-Lucas, M. Abdelwahab, and C. Busso, "The MSP-conversation corpus," in *Interspeech*, Shanghai, China, Oct. 2020.
- [32] R. Lotfian and C. Busso, "Building naturalistic emotionally balanced speech corpus by retrieving emotional speech from existing podcast recordings," *IEEE Tran. on Affective Computing*, vol. 10, no. 4, pp. 471–483, Dec. 2019.
- [33] F. Ringeval, A. Sonderegger, J. Sauer, and D. Lalanne, "Introducing the RECOLA multimodal corpus of remote collaborative and affective interactions," in *IEEE Int. Conf. and Workshops on Automatic Face and Gesture Recognition (FG)*, Shanghai, China, Apr. 2013.

- [34] J. Kossaifi, R. Walecki, Y. Panagakis, J. Shen, M. Schmitt, F. Ringeval, J. Han, V. Pandit, A. Toisoul, B. Schuller *et al.*, "Sewa db: A rich database for audio-visual emotion and sentiment research in the wild," *IEEE Trans., on pattern analysis and machine intelligence*, vol. 43, no. 3, pp. 1022–1040, 2019.
- [35] N. Raj Prabhu, C. Raman, and H. Hung, "Defining and Quantifying Conversation Quality in Spontaneous Interactions," in *Comp. Pub. of 2020 Int. Conf. on Multimodal Interaction*, Sep. 2020.
- [36] D. Gatica-Perez, "Automatic nonverbal analysis of social interaction in small groups: A review," *Image and Vision Computing*, vol. 27, no. 12, pp. 1775–1787, Nov. 2009.
- [37] M. Valstar, J. Gratch, B. Schuller, F. Ringeval, D. Lalanne, M. Torres Torres, S. Scherer, G. Stratou, R. Cowie, and M. Pantic, "AVEC 2016: Depression, Mood, and Emotion Recognition Workshop and Challenge," in *Proc., of the 6th Int., Workshop on Audio/Visual Emotion Challenge*, New York, NY, USA, 2016.
- [38] N. Raj Prabhu, G. Carbajal, N. Lehmann-Willenbrock, and T. Gerkmann, "End-to-end label uncertainty modeling for speech-based arousal recognition using Bayesian neural networks," in *Inter-speech*, Incheon, Korea, September 2022.
- [39] N. Raj Prabhu, N. Lehmann-Willenbrock, and T. Gerkmann, "Label uncertainty modeling and prediction for speech emotion recognition using t-distributions," in *IEEE Int. Conf. on Affective Computing and Intelligent Interaction*, Nara, Japan, Oct. 2022.
- [40] M. Abdelwahab and C. Busso, "Active learning for speech emotion recognition using deep neural network," in *IEEE Int. Conf. on Affective Computing and Intelligent Interaction*, Cambridge, UK, Sep. 2019.
- [41] S. Steidl, M. Levit, A. Batliner, E. Noth, and H. Niemann, "'of all things the measure is man" automatic classification of emotions and inter-labeler consistency," in *IEEE Int. Conf. on Acoustics, Speech, Sig. Proc., ICASSP*, Philadelphia, USA, 2005.
- [42] H. M. Fayek, M. Lech, and L. Cavedon, "Modeling subjectiveness in emotion recognition with deep neural networks: Ensembles vs soft labels," in *IEEE Int., Joint Conf., on Neural Networks (IJCNN)*, Vancouver, Canada, Jul. 2016.
- [43] L. Tarantino, P. N. Garner, and A. Lazaridis, "Self-attention for speech emotion recognition," in *Interspeech*, Graz, Sep. 2019.
- [44] J. Han, Z. Zhang, M. Schmitt, M. Pantic, and B. Schuller, "From hard to soft: Towards more human-like emotion recognition by modelling the perception uncertainty," in *Proc., of the 25th ACM Int. Conf. on Multimedia*, Mountain View, USA, Oct. 2017.
- [45] T. Dang, V. Sethu, and E. Ambikairajah, "Dynamic multi-rater gaussian mixture regression incorporating temporal dependencies of emotion uncertainty using kalman filters," in *IEEE Int. Conf. on Acoustics, Speech, Sig. Proc., ICASSP*, Calgary, Canada, Apr. 2018.
- [46] G. Rizos and B. Schuller, "Modelling sample informativeness for deep affective computing," in *IEEE Int. Conf. on Acoustics, Speech, Sig. Proc., ICASSP*, Brighton, UK, May 2019.
- [47] H.-C. Chou, W.-C. Lin, C.-C. Lee, and C. Busso, "Exploiting annotators' typed description of emotion perception to maximize utilization of ratings for speech emotion recognition," in *IEEE Int. Conf. on Acoustics, Speech, Sig. Proc., ICASSP*, Singapore, Jan. 2022.
- [48] R. E. Walpole, R. H. Myers, S. L. Myers, and K. Ye, *Probability & statistics for engineers and scientists*. Pearson Education, 2007.
- [49] C. Villa and S. G. Walker, "Objective prior for the number of degrees of freedom of at distribution," *Bayesian Analysis*, vol. 9, no. 1, pp. 197–220, 2014.
- [50] I. Goodfellow, Y. Bengio, and A. Courville, *Deep Learning*, 3rd ed., ser. 5. MIT Press, Jul. 2016, vol. 4, ch. 3, pp. 51–77.
- [51] S. Kullback and R. A. Leibler, "On information and sufficiency," *The annals of mathematical statistics*, vol. 22, no. 1, pp. 79–86, 1951.
- [52] K. P. Murphy, *Machine learning : a probabilistic perspective*. Cambridge, USA: MIT Press, 2012.
- [53] A. Paszke, S. Gross, F. Massa, A. Lerer, J. Bradbury, G. Chanan, T. Killeen, Z. Lin, N. Gimelshein, L. Antiga *et al.*, "Pytorch: An imperative style, high-performance deep learning library," in *Advances in Neural Inf. Proc. Sys., NeurIPS*, Vancouver, Dec. 2019.
- [54] D. Rees, "Essential statistics," *American Statistician*, vol. 55, 2001.
- [55] P. Tzirakis, A. Nguyen, S. Zafeiriou, and B. W. Schuller, "Speech emotion recognition using semantic information," in *IEEE Int. Conf. on Acoustics, Speech, Sig. Proc., ICASSP*, Toronto, Jun. 2021.
- [56] S. Butterworth *et al.*, "On the theory of filter amplifiers," *Wireless Engineer*, vol. 7, no. 6, pp. 536–541, 1930.
- [57] J. W. Cooley and J. W. Tukey, "An algorithm for the machine calculation of complex fourier series," *Mathematics of computation*, vol. 19, no. 90, pp. 297–301, 1965.

[58] K. Sridhar and C. Busso, "Unsupervised personalization of an emotion recognition system: The unique properties of the externalization of valence in speech," *IEEE Transactions on Affective Computing*, pp. 1–17, Jun. 2022.

[59] F. Eyben, K. R. Scherer, B. W. Schuller, J. Sundberg, E. André, C. Busso, L. Y. Devillers, J. Epps, P. Laukka, S. S. Narayanan *et al.*, "The Geneva minimalistic acoustic parameter set (GeMAPS) for voice research and affective computing," *IEEE Tran. on Affective Computing*, vol. 7, no. 2, pp. 190–202, Jul. 2015.



speech signal processing, and group affect.

Navin Raj Prabhu received a B.Tech degree in Computer Science from SRM University, India, in 2015, and the MS degree in Computer Science from the Intelligent Systems Department at the Delft University of Technology, Delft, The Netherlands, in 2020. Currently, he is a PhD student at the Signal Processing Lab and Organisation Psychology Lab, University of Hamburg, Hamburg, Germany. His research interests include affective computing, social signal processing, deep learning, uncertainty modelling,



studies emergent behavioral patterns in organizational teams, social dynamics among leaders and followers, and meetings at the core of organizations. Her research program blends organizational psychology, management, communication, and social signal processing. She serves as associate editor for the Journal of Business and Psychology as well as for Small Group Research.

Nale Lehmann-Willenbrock studied Psychology at the University of Goettingen and University of California, Irvine. She holds a PhD in Psychology from Technische Universität Braunschweig (2012). After several years working as an assistant professor at Vrije Universiteit Amsterdam and Associate Professor at the University of Amsterdam, she joined Universität Hamburg as a full professor and chair of Industrial/Organizational Psychology in 2018, where she also leads the Center for Better Work. She



Sound and Image Processing Lab at the Royal Institute of Technology (KTH), Stockholm, Sweden. From 2011 to 2015 he was a professor for Speech Signal Processing at the Universität Oldenburg, Oldenburg, Germany. During 2015 to 2016 he was a Principal Scientist for Audio & Acoustics at Technicolor Research & Innovation in Hanover, Germany. Since 2016 he is a professor for Signal Processing at the Universität Hamburg, Germany. His main research interests are on statistical signal processing and machine learning for speech and audio applied to communication devices, hearing instruments, audio-visual media, and human-machine interfaces. Timo Gerkmann serves as an elected member of the IEEE Signal Processing Society Technical Committee on Audio and Acoustic Signal Processing and as an Associate Editor of the IEEE/ACM Transactions on Audio, Speech and Language Processing. He received the VDE ITG award 2022.

Timo Gerkmann (S'08–M'10–SM'15) studied Electrical Engineering and Information Sciences at the Universität Bremen and the Ruhr-Universität Bochum in Germany. He received his Dipl.-Ing. degree in 2004 and his Dr.-Ing. degree in 2010 both in Electrical Engineering and Information Sciences from the Ruhr-Universität Bochum, Bochum, Germany. In 2005, he spent six months with Siemens Corporate Research in Princeton, NJ, USA. During 2010 to 2011 Dr. Gerkmann was a postdoctoral researcher at the